Hindawi
Shock and Vibration
Volume 2021, Article ID 6664188, 14 pages
https://doi.org/10.1155/2021/6664188

Research Article

Optimal Three-Dimensional Sensor Placement for Cable-Stayed Bridge Based on Dynamic Adjustment of Attenuation Factor Gravitational Search Algorithm

Bo Gao, Zhihui Bai, and Yubo Song

School of Mechatronic Engineering, Lanzhou Jiaotong University, Lanzhou 730070, China

Correspondence should be addressed to Bo Gao; gaobo@mail.lzjtu.cn

Received 9 November 2020; Revised 7 February 2021; Accepted 22 February 2021; Published 31 March 2021

Academic Editor: Yaobing Zhao

Structural health monitoring (SHM) is essential when detecting damage in large and complex structures in order to provide a comprehensive assessment of the structural health state. Optimal sensor placement (OSP) is critical in the structural health monitoring system, which aims to use a limited number of sensors to obtain high-quality structural health diagnosis data. However, the current research mainly focuses on OSP for structures, without considering the values contributed by different modes to the bridge structure. In this article, an optimal sensor placement method based on initial sensor layout, using the dynamic adjustment of attenuation factor gravitational search algorithm (DGSA), is proposed. The effective modal mass participation ratio is introduced to ensure the validity of the initial data of optimal sensor placement. In view of the insufficient developmental ability of the gravitational search algorithm, the attenuation factor α adjusted dynamically aids the global search in the early iteration and the local fine search in the late iteration. The double coding method is used to apply the DGSA algorithm to OSP; taking cable-stayed bridges as an example, the feasibility of the algorithm is verified. The results show that the improved algorithm has a good optimization ability and can accurately and efficiently determine the optimal placement of sensors.

1. Introduction

With the progress being made in science and technology, large buildings and bridge structures are becoming widely used. When they are subjected to harsh environments and extreme events, such as strong winds and severe earthquakes, the functionality and safety of the large structures become a vital issue, and structural health monitoring (SHM) technology has been developed for damage detection [1]. SHM uses nondestructive sensing technology to analyze the system characteristics through the detected response, achieving the purpose of monitoring the structural health state, or predicting the service life, of the structure. In the SHM system, the main tasks of the sensor system include real-time acquisition of the operating environment of the structure, the load on the structure, and the dynamic characteristics of the structure [2, 3]. When the number of sensors is large, the monitoring cost will increase. When there are few sensors, the measurement data will be incomplete, and the measurement result will be unreasonable. Therefore, adopting an optimal sensor placement scheme to obtain maximal structural information is critical in health monitoring.

In the optimal sensor placement method, the traditional optimization algorithm is incorporated with one of the following: the effective independence method [4–6], the Guyuan reduction method [7], the modal kinetic energy method [8, 9], and the information entropy method [10, 11]. The above mentioned traditional methods have difficulties in obtaining their global or near-global optimum. In recent years, many optimal sensor placement methods based on intelligent algorithms have been proposed, such as the genetic algorithm (GA) [12, 13], the monkey algorithm (MA) [14], the harmony search (HS) algorithm [15], the sequence algorithm (SA) [16], the particle swarm optimization (PSO) algorithm [17], and the differential evolution algorithm (DE)

[18]. For the objective function, the modal assurance criterion (MAC) is widely used to quantify the collinearity between the modal shape vectors placed by the sensors. The strategy involves minimizing the nondiagonal term of the MAC matrix to distinguish the modal shapes.

Many researchers have attempted to improve the efficiency and performance of sensor optimization methods. Zhou et al. [19] proposed a one-dimensional binary coding method, which was applied in the optimal arrangement of cable-stayed bridge sensors. Yi et al. [12] improved the genetic algorithm and used the double structure coding method to optimize sensor placement in high-rise buildings. Yi et al. [14] introduced the adaptive operator into the monkey algorithm, increased the global search ability of the algorithm, and took the modal assurance criterion as the objective function, and the optimization is thus achieved through the experimental analysis. Jin et al. [15] combined the harmony search (HS) algorithm with the modal assurance criterion and applied it to sensor placement on a gantry crane. The results show that the HS algorithm is a powerful search and optimization algorithm. Yin et al. [16] used the concept of Dijkstra's edge relaxation operation to generate the initial solution set from the sequence algorithm and improved this set via relaxation until the end of the relaxation operation. Taking the truss structure as an example, the effectiveness of the algorithm was verified. Although the abovementioned swarm intelligence algorithm can be applied to sensor layout optimization, it has the disadvantages of poor robustness, insufficient development ability, and more control parameters.

Although the above mentioned research has made significant achievements, there are still three aspects that have not been considered. Firstly, many sensor optimization methods do not consider the mode selection but select the first few modes based on experience, which may not fully reflect the information of the mechanism due to improper mode selection. Secondly, many researchers do not consider the relationship between the number of sensors and the objective function but give a set of sensor layout schemes for a given number of sensors. Third, there are many nodes to be measured in the optimal sensor layout. Figuring out how to use OSP to solve high-dimensional problems with high accuracy and efficiency is still a challenge. Therefore, an innovative method is needed to accurately and effectively determine OSP in the structure.

In view of these three defects, a reworking of the dynamic adjustment of attenuation factor gravitational search algorithm (DGSA) is presented in this paper. The cumulative effective modal participation ratio is the percentage of the modal effective mass to the total mass. This concept has been successfully applied in seismic design and the optimal placement of bridge sensors in order to determine the number of main modes [13, 17, 20]. In this paper, the effective modal mass participation ratio is used to select the main modal of a bridge. In order to improve the performance and search ability of the gravitational search algorithm (GSA), this paper improves the GSA by adjusting the attenuation factor α, of the gravitational constant$G$, to change the step lengths of particles in different periods. The improved DGSA offers greater precision and a faster convergence speed. The specific content of this paper is as follows: Section 2 introduces the improved GSA, Section 3 introduces the optimal sensor placement method based on the DGSA, and Section 4 takes a cable-stayed bridge as the object, reports on the example test, and offers an analysis of its results. Section 5 contains the conclusion and future work arrangement.

2. DGSA Algorithm

The gravitational search algorithm utilizes the gravitational attraction between particles. The particle with the largest mass in the given population occupies the optimal position, and the other particles move towards the particle with the highest mass under the action of gravity; thus, the process of obtaining the global optimal solution of the problem is carried out. There are M particles in the algorithm. Taking one of the particle i as an example, the particle i is subjected to the gravitational attraction of the other particles, and acceleration a and velocity v are generated under this combined force, such that in the ensuing moments, the particle i approaches the global optimal solution. The gravitational constant runs through the entire search process of the algorithm from the beginning to end. The change process of the G value directly affects the search efficiency and optimization precision of the algorithm. The value of the attenuation factor α in the GSA is constant, which causes the particles to move with fixed step sizes in the process of searching, making it easy for the algorithm to reach the local extreme point. In order to enhance the optimization ability of the algorithm, the DGSA proposed in this paper adaptively adjusts α. At the beginning of the search, the particle is far away from the optimal solution and searches globally with a larger step size. At a later stage of the search, the particle is in closer proximity to the optimal solution and employs smaller step sizes in searching, which is conducive to the local search of the algorithm and to effectively finding the global optimal solution.

2.1. Gravity Search Algorithm. GSA [21], with its advantages of easy implementation, good operability, and obvious optimization effect, has been widely used in production practice [22–24].

Assuming the population number is N, the position of particle i in the Wdimensional space is$X_i = [x_i^1, \ldots, x_i^d, \ldots x_i^W]$, where $(i = 1, 2, \ldots, N)$. Then, the gravitational attraction of particle i and particle j in the Wdimensional space at time t is defined as

$$F_{ij}^d(t) = G(t)\frac{M_i(t) * M_j(t)}{D + \varepsilon}\left(x_i^d(t) - x_j^d(t)\right), \quad (1)$$

where $M_i(t)$ is the gravitational mass related to particle i, $M_j(t)$ is the gravitational mass related to particle j, $G(t)$ is the gravitational constant at time t, ε is a small constant, and D is the Euclidian distance between two agents i and j.

Formula for calculating $G(t)$ is defined as

$$G(t) = G_0 e^{-(\alpha * I/I_{\max})}, \tag{2}$$

where I is the number of the iterations and $I_{\max}$ refers to the maximum number of iterations.

The resultant force $F_i^d(t)$ of particle i in d dimensional space is defined as

$$F_i^d(t) = \sum_{j \in \text{best}} \text{rand} * F_{ij}^d(t), \tag{3}$$

where *best* is a collection of particles that have gravitational effects on particle i.

The acceleration $a_i^d(t)$ of particle i is defined as

$$a_i^d(t) = \frac{F_i^d(t)}{\text{Mass}_i(t)} = \frac{\sum_{j \in \text{best}} \text{rand} * F_{ij}^d(t)}{\text{Mass}_i(t)}, \tag{4}$$

where $\text{Mass}_i(t)$ is the inertia mass of particle i, and its formula is defined as

$$m_i(t) = \frac{\text{fit}_i(t) - \text{fit}_w(t)}{\text{fit}_b(t) - \text{fit}_w(t)}, \tag{5}$$

$$\text{Mass}_i(t) = \frac{m_i(t)}{\sum_{j=1}^{n} m_i(t)}, \tag{6}$$

where $\text{fit}_b(t)$ represents the best fitness value and $\text{fit}_w(t)$ represents the worst fitness value.

The formula for the velocity and position of the particle i at the next moment is

$$\begin{cases} v_i^d(t) = \text{rand} * v_i^d(t) + a_i^d(t), \\ x_i^d(t+1) = x_i^d(t) + v_i^d(t+1). \end{cases} \tag{7}$$

Note 1:rand is a random variable which is uniformly distributed among [0, 1].

2.2. Dynamic Adjustment of Attenuation Factor Gravitational Search Algorithm. The gravitational constant, $G(t)$, has a significant influence over the convergence speed and optimization precision of the algorithm. The αin formula (2) has the effect of adjusting the convergence speed of the algorithm. Aiming at the optimization efficiency and search accuracy of GSA, this paper improves the GSA and proposes the DGSA. Considering that the value of α in the GSA is a constant, in the iterative process of the algorithm, regardless of whether the particle is far from or near to the global optimal solution, the particle moves with a fixed step size. As a result, when the particle is far away from the optimal solution, its step length is too small, it moves too slowly, and it takes too long. Furthermore, when the particle is close to the optimal solution, the step length is too large, which may cause it to deviate from the optimal solution and fall into the local optimal solution. Therefore, DGSA selects a smaller attenuation factor α in the early stage of the search, and the particles perform the global search with a larger step size, which is beneficial in reducing the search time of the algorithm and improving the overall optimization efficiency. The algorithm selects a larger attenuation factor α in the later stage, and the particles employ a smaller step size to complete the local search, so as to avoid the algorithm falling upon the local extreme point. The expression of adaptive attenuation factor α is defined as

$$\alpha(t) = \beta * e^{-\left|1 - t/I_{\max}\right|}, \tag{8}$$

where t represents the current number of iterations and β is the initial parameter. According to experience, when $\beta = 1$, the optimization effect of the algorithm is the best. The schematic diagram of the DGSA is shown in Figure 1.

Particle M_1 generates resultant force F_1 and acceleration a_1 under the action of universal gravitation of M_2, M_3, and M_4. Through the adaptive mechanism of attenuation factorα, particle M_1 approaches the global optimal solution with different steps.

3. Optimal Sensor Placement Based on DGSA Method

In this section, the dual-structure coding method is used to solve the problem of DGSA being unable to realize optimal sensor placement, and the flow of optimal sensor placement is shown in Figure 2. In the mode selection, by calculating the effective modal mass participation ratio, the mode order with a larger contribution value is selected.

3.1. Modal Assurance Criterion. The existing sensor optimization approaches, such as the modal kinetic energy method, are highly dependent on the accuracy of the finite element mesh, which will affect the reliability of the data. It is easy to lose the mode to be measured when using the Guyan reduction method, which increases the difficulty of identification. The modal assurance criterion is one of the most widely used evaluation criteria for optimal sensor placement. It can enable the choosing of a larger space intersection angle and can retain the characteristics of the original model as much as possible.

3.1.1. Mode Selection. The selection of mode is the premise to determine the number of sensors and then determine the location of sensor. If too many modes are selected, not only a lot of calculation time and space will be consumed but also it is difficult to accurately define the correctness of the calculation results. If too few modes are selected, the reliability of the optimal sensor placement results will be too small to represent the complete information of the bridge. At present, many scholars have applied the effective modal mass participation factor to the selection of the modal order and calculated it by using the ratio of the influence of the current modal mass to the influence of all modal masses.

The dynamic formula of n-DOF system is expressed as

$$M\ddot{u} + C\dot{u} + Ku = -Me\ddot{u}_a(t), \tag{9}$$

where M is the mass matrix, C is the damping matrix, K is the stiffness matrix, e is the direction matrix under the excitation force, $\ddot{u}_a(t)$ is the acceleration produced by the

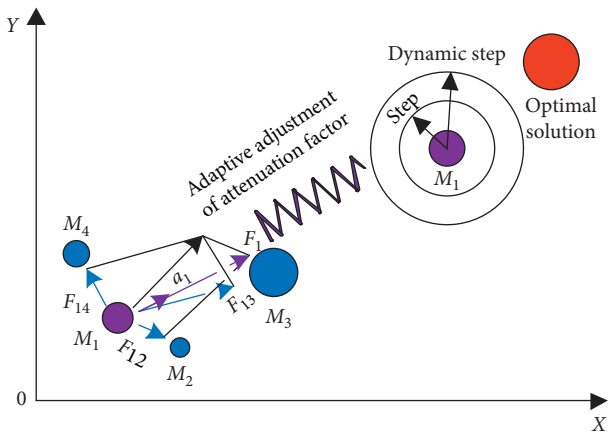

Figure 1: Schematic diagram of DGSA.

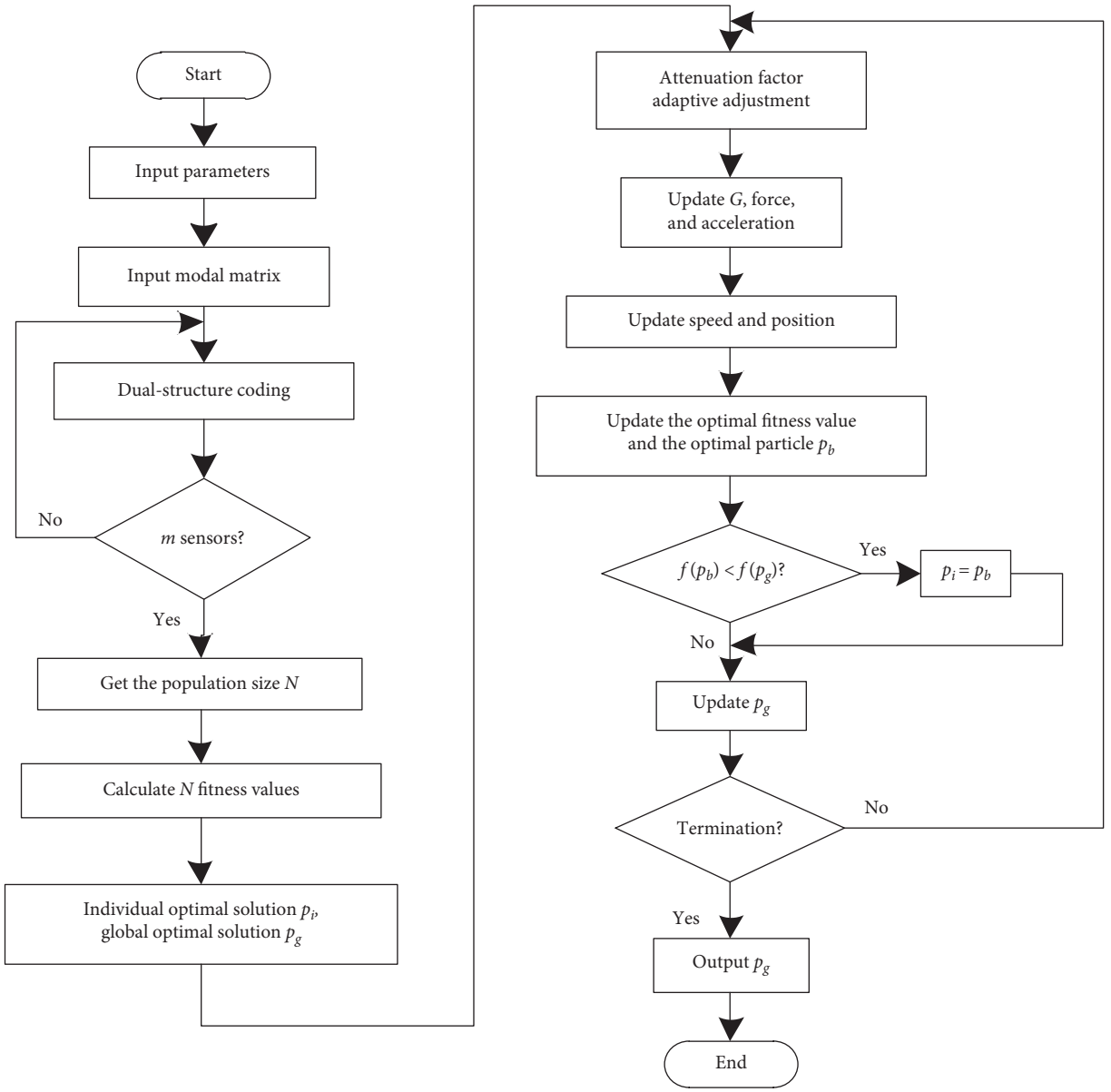

Figure 2: Optimal sensor placement based on DGSA.

excitation force, u, $\dot{u}$, and $\ddot{u}$ are modal displacement responses, velocity response, and acceleration response, respectively.

The relationship between the abovementioned response and the mode shape matrix ϕ is as follows:

$$u = \phi \cdot q, \dot{u} = \phi \cdot \dot{q}, \ddot{u} = \phi \cdot \ddot{q}. \tag{10}$$

Based on the orthogonality of M, C, and K, we can get the following formula from (9) and (10):

$$\ddot{q}_i + 2\xi_i \omega_i \dot{q}_i + \omega_i^2 q_i = -\frac{\phi_i^T M e}{\phi_i^T M \phi_i} \ddot{u}_a(t), \tag{11}$$

where q_i is the modal coordinates, ω_i is the natural frequency of the structure, and ξ_i is the modal damping ratio.

The participation factor is defined by the following:

$$\sigma_i = \frac{\phi_i^T M e}{\phi_i^T M \phi_i}. \tag{12}$$

According to the principle of mass normalization of mode shape matrix ϕ_i, the following formula is obtained:

$$\phi_i^T M \phi = 1. \tag{13}$$

Then, formula (12) can be converted into the following:

$$\sigma_i = \phi_i^T M e. \tag{14}$$

The effective modal mass expression of the ith mode is

$$M_i = \frac{\sigma_i^2}{\phi_i^T M \phi_i}. \tag{15}$$

Therefore, the total modal mass is

$$\sum_{i=1}^{n} M_i = \sum_{i=1}^{n} \sigma_i^2 = \sigma^T \sigma. \tag{16}$$

The expression of the ith order effective mode mass participation ratio r_i is

$$r_i = \frac{M_i}{e^T M e}. \tag{17}$$

For the first m modes ($m < n$), the total modal mass participation ratio R of the first m modes is

$$R = \sum_{i=1}^{m} r_i. \tag{18}$$

According to the research, when the value of R is more than 90%, it shows that the selected modal order contains enough structural information, which can be used as the mode shape of optimal sensor placement.

3.1.2. Fitness Function. The most important step in the problem of optimal sensor placement is to establish the mathematical model of the structure and construct the objective function. Actually, due to the external factors, the accuracy error of the measuring instrument and the noise interference of the test site, the included angle of the modal vector is too small, or even 0, which leads to the loss of modal information. Therefore, the optimal sensor placement should select the points with large modal angle and be easy to identify. The modal assurance criterion (MAC) is usually used to compare the correlation and independence of experimental modes [25–27], so MAC can be used as the fitness function of optimal sensor placement to evaluate the independence of each mode.

The expression of MAC is as follows:

$$MAC_{ij} = \frac{\left(\phi_i^T \cdot \phi_j\right)^2}{\left(\phi_i^T \cdot \phi_i\right)\left(\phi_j^T \cdot \phi_j\right)}, \tag{19}$$

where ϕ_i and ϕ_j represent the ith and jth column vectors in matrixϕ.

In the above formula, maximum off-diagonal element ranges from 0 to 1. The smaller the maximum off-diagonal element means the larger the corresponding space angle and the easier to distinguish the modal vectors. The smaller the value of the off-diagonal element of the MAC matrix, the better the calculated modal vector independence and the easier it is to identify the mode shape. Therefore, the minimization of the maximum off-diagonal element of MAC matrix can be taken as the fitness function of optimal sensor placement of bridge, and the expression is as follows:

$$\text{fit} = \min f(x), \tag{20}$$

where $f(x) = \max_{i \neq j} |MAC_{ij}|$. The smaller the value of the objective function, the better the independence of the tested modal vector and the better the optimal sensor placement.

3.2. Method of Coding. The binary coding method can be used to solve the optimal sensor placement problem; 1 indicates the sensor is placed, and 0 indicates the sensor is not placed, but this coding method will lead to changes in the number of sensors. Here, dual-structure coding is adopted to overcome this problem. The dual-structure coding method is shown in Table 1.

The dual-structure coding method involves extra code and variable code. The extra code represents the position vector of the individual, and the variable code represents binary vector 0 or 1, where 0 means no sensor is placed, and 1 means placement of sensor. This dual coding method enables the DGSA to solve the problem of optimal sensor placement. For example, there are known to be nine points that must be selected. The dual-structure coding results are shown in Table 2. The sensor arrangement we were able to derive is s = (3, 4, 6, 8).

3.3. Optimal Sensor Placement Process Based on DGSA

Step 1. Select and import mode matrix. The order choice of the mode matrix has an important influence on the sensor placement results. On the one hand, the appropriate mode matrix can represent the overall performance of the structure and ensure the accuracy of the optimal sensor placement. On the other hand, the optimal sensor placement is

Table 1: Dual-structure coding method.

Extra code	$x(1)$	$x(2)$	$\cdots$	$x(i)$	$\cdots$	$x(f)$
Variable code	$s_x(1)$	$s_x(2)$	$\cdots$	$s_x(i)$	$\cdots$	$s_x(f)$

Table 2: The result of dual-structure coding method.

Extra code	5	3	6	1	4	7	2	8
Variable code	0	1	1	0	1	0	0	1

different with different modes. The first and foremost, the mode shape matrix of all nodes of the model is obtained by mode analysis method, and the obtained mode shape matrix is taken as the input value, and the degrees of freedom corresponding to all nodes are used as the candidate points of the optimal sensor placement. Secondly, assuming that the number of candidate points is n and the number of sensors is m, the n candidate positions are numbered from 1 to n successively.

Step 2. Taking the ith particle in the population as an example, ($i = 1, 2, \ldots, N$, in which N is the number of population size), the corresponding solution to i can be expressed as $xs(i) = (x_i, s_i) = \{(x_{i1}, s_{i1})(x_{i2}, s_{i2}), \ldots, (x_{in}, s_{in})\}$. The position vectors of x_i are obtained by formula (21), and the binary vectors of s_i are obtained by formula (22), where $x_{\text{down}} = -8$, $x_{\text{up}} = 8$,

$$x_{ij} = \text{rand} \times \left(x_{\text{up}} - x_{\text{down}}\right) + x_{\text{down}}, \tag{21}$$

where rand is a random number between 0 and 1.

$$s_{ij} = \left| \frac{x_{ij}}{\sqrt{1 + x_{ij}^2}} \right|, \tag{22}$$

In formula (22), the binary vectors calculated by different position components x_{ij} are different, so a threshold δ needs to be set to satisfy the following:

$$s_{ij} = \begin{cases} 1, & \text{if } V\left(x_{ij}\right) > \delta, \\ 0, & \text{else}, \end{cases} \tag{23}$$

where $j \in \{1, 2, \ldots, n\}$, $\delta = 0.5$, and the components of each position of x_{ij} are substituted into formula (23). If the function value is greater than 0.5, the additional code value is 1, indicating that the sensor is placed at this candidate point. If the function value is less than 0.5, the additional code value is 0, indicating that the sensor is not placed at this candidate point. It can be obtained by calculation that the value of x_{ij} is taken as $[-8, 8]$, and the value of s_{ij} is $0 \le V(x_{ij}) \le 0.9923$. It can be approximated instead of $[0, 1]$.

Step 3. Repeat Steps 1 and 2 until N particles are generated; during initialization, the total number of sensors in s_i is not equal to the number of sensors arranged m. In order to ensure that all possible solutions in the population meet the requirements, when we encounter this problem, we should reinitialize at this time, and repeat Step 2 until the initial solution meets the requirements of coding.

Step 4. The N particles in the population are substituted into formula (20). The best fitness value is labeled $\text{fit}_b(xs_i)$, and the worst fitness value is labeled $\text{fit}_w(xs_i)$. The optimal arrangement corresponding to the fitness value is recorded as $p_i(xs_i)$, $p_i(xs_i)$ represents the individual optimal solution of particles in the population, and it is the optimal solution in each particle iteration. $p_g(xs_i)$ represents the global optimal solution, which is the optimal solution among all particles in the population.

Step 5. The inertia mass of each particle is calculated using formulas (5) and (6). Adaptively change the attenuation factor α according to formula (2) and update the gravitational constant $G(t)$.

Step 6. Taking particle i as an example, the corresponding position component is $x_i = \{x_{i1}, x_{i2}, \cdots, x_{im}\}$, where m is the number of sensors that need to be arranged, and the Euclidean distance between the particle i and other particles is calculated. Using formulas (1) and (3), the resultant force of particle i under the action of other particles is obtained. Using formula (4) to calculate the acceleration of particle i, similarly, the gravitational and acceleration forces of other particles in the population are calculated.

Step 7. In order to speed up the convergence of particles, improve the optimization performance. The mutation operator is introduced into the velocity formula of the particle to increase the guiding effect of the current optimal solution and the global optimal solution on the particle and improve the convergence speed of the algorithm. The expression of the mutation operator is as in formula (8). In the process of updating the speed and position, the calculated acceleration component and velocity component may appear as non-integer. Therefore, we round the speed formula and the position formula. The specific expression is as follows:

$$\eta = \text{rand}\left(p_g^d(t) - x_i^d(t)\right), \tag{24}$$

$$\begin{cases} v_i^d(t) = \text{round}\left(\text{rand} \times v_i^d(t) + a_i^d(t) + \eta\right), \\ x_i^d(t+1) = \text{round}\left(x_i^d(t) + v_i^d(t+1)\right), \end{cases} \tag{25}$$

where the round is a function to ensure that the updated particle position component is an integer. The positional component of the particle is an integer randomly generated from $[-8, 8]$. In Step 7, the particle may exceed the range of values in the position update. Therefore, this paper stipulates that when the position component is greater than 8, it takes 8; when the position component is less than -8, it takes -8.

Step 8. Substituting the mode displacement corresponding to the updated particle into formula (20), if the updated fitness value is less than before the update, the particle position changes. Otherwise, the particle position remains unchanged. The optimal placement corresponding to the

updated optimal fitness value is denoted as $p_b(xs_i)$. If the updated optimal fitness value $\text{fit}(p_b(xs_i))$ is smaller than the fitness value $\text{fit}(p_g(xs_i))$ corresponding to the global optimal value $p_g(xs_i)$ of the previous generation, the current particle is used instead of the global optimal solution. Otherwise, the global optimal solution remains unchanged.

Step 9. Determine whether the algorithm reaches the preset accuracy requirement or the maximum number of iterations. If it is satisfied, stop the iteration and output the global optimal solution, which is the required sensor placement; if not, return to Step 6. The flow chart based on DGSA is shown in Figure 2.

4. Model Validation

In this section, the DGSA will be used in the optimal sensor placement on the test object, so as to verify the feasibility and effectiveness of this algorithm.

4.1. Modeling and Modal Analysis. The example selected in this paper is a single-tower cable-stayed bridge with a total length of 264 m. Its main components include a main beam, a bridge tower, and a stay cable. ANSYS 19.2 was used to establish the finite element model of the bridge, as shown in Figure 3. Through modal analysis, the model was determined to have 1588 nodes and 2422 elements; each node incorporates three degrees of freedom, corresponding to the modal information of the x, y, and z directions. Figures 4–6 show the effective modal mass corresponding to the first 50 modes of the cable-stayed bridge in the x, y, and z directions, respectively.

4.2. Mode Number. Considering that the selection of mode is very important in the optimal placement of sensors, a matrix of the first 50 modes of the cable-stayed bridge is derived through the modal analysis process. The effective modal mass participation ratio in three directions is calculated, and the modal order with an R value greater than 90% is selected as the mode to be used. The effective mass corresponding to the first 50 modes is shown. The main modes are selected in the x, y, and z directions, and the corresponding M_i, r_i, and R are determined.

Three and four modes with high effective participation mass, and twelve modes in total, are selected in the x, y, and z directions, respectively, and the corresponding values of R and the other parameters are shown in the table. It can be seen from Table 3 that the value of R for the 12 modes is 0.9235; the value of R for the first 8 modes is 0.8335, and the value of R for the last 4 modes is 0.0900. The R values of the 2nd, 3rd, 6th, 9th, 11th, 16th, 30th, and 48th modes occupy the main part of the 12th mode in the table, which can be used as the main mode to represent the information of the cable-stayed bridge. Therefore, the 2nd, 3rd, 6th, 9th, 11th, 16th, 30th, and 48th modes are chosen as the initial modes of the optimal sensor placement.

4.3. Analysis of the Sensor Placement Results

4.3.1. Number of Sensors. Generally speaking, the higher the number of sensors arranged, the greater the amount of obtainable information pertaining to structural arrangement, and the better the reflection of the structure's health condition. However, in practical applications, because of the high cost of sensors, having a very high number of sensors is often impossible, so the selection of the number of sensors is very important. Therefore, this paper takes the number of sensors as the independent variable and formula (20) as the objective function. Each group of variables is calculated 10 times, and the average value of the results of 10 operations is the corresponding variable.

It can be seen that when the optimal sensors quantity is between 1 and 11, the decline curve of the objective function is steeper. When the number of sensors is 11, the value of the objective function is the lowest. When the number of sensors changes from 11 to 12, the value of the objective function begins to increase. When the number is between 12 and 30, the value of the objective function begins to decrease slowly and tends to be stable. Considering the cost of the sensors, $m = 11$ is selected as the optimal number of sensors.

4.3.2. Optimizing Performance Comparison. Optimal sensor placement is performed according to the DGSA proposed in this paper, with the following parameters: population size $N = 100$, maximum iteration times $I_{\max} = 100$, initial value of gravitational constant $G_0 = 100$, and attenuation factor $\beta = 40$. When the number of sensor m is 7, 11, and 15, the algorithm repeats 10 times to calculate the optimal solution, the worst solution, and the average solution of the objective function.

Figure 7 shows the curve of the objective function changing with the number of sensors when other parameters are unchanged. It can be seen from Figures 8–10 that the fitness function values corresponding to different numbers of sensor are different. When the number of sensor m arranged is 7, 11, and 15, respectively, the average values of the objective function are 0.1866, 0.0526, and 0.0489. The results show that with the increase of m, the smaller the average value of the objective function, the easier to identify the modal vector obtained by the search, and the optimal value of the objective function can reach 0.1815, 0.0410, and 0.0455 in turn. It shows that within a certain value range, as the number of sensor increases, the sensor placement results can be better.

In order to further highlight the advantages of the DGSA, the results of the DGSA, the GA algorithm, and the PSO algorithm are compared when 11 sensors are arranged. Figure 11 shows the performance curve comparison for the three algorithms. In the case of 100 iterations of three algorithms, the convergence speed and optimization accuracy of the DGSA are better than those of the GA and PSO. Among them, GA, PSO, and DGSA are different parameters, and the optimal solution is obtained after many repetitions of the verification procedure.

Figures 12–14 show a bar chart of the MAC matrices for the three algorithms. The maximum values of the off-diagonal element of the MAC matrix obtained by the GA algorithm and the PSO algorithm are 0.0741 and 0.0694,

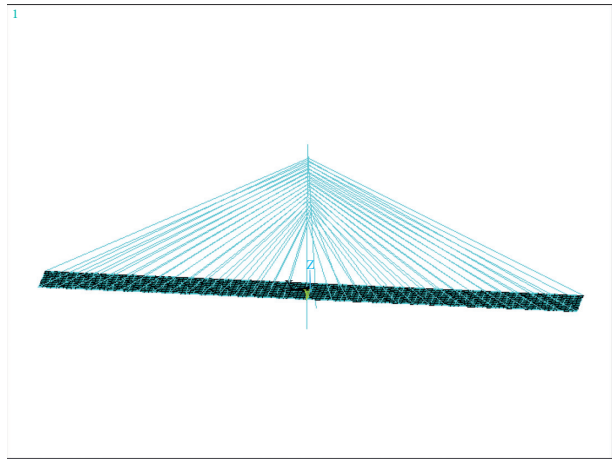

Figure 3: Cable-stayed bridge model.

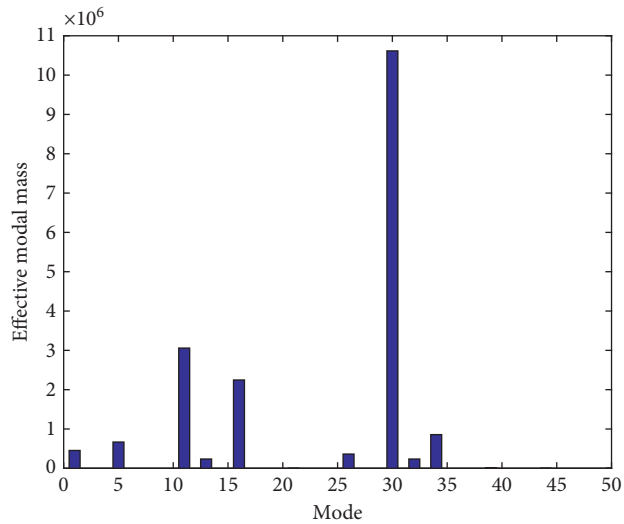

Figure 4: Effective modal mass in x direction.

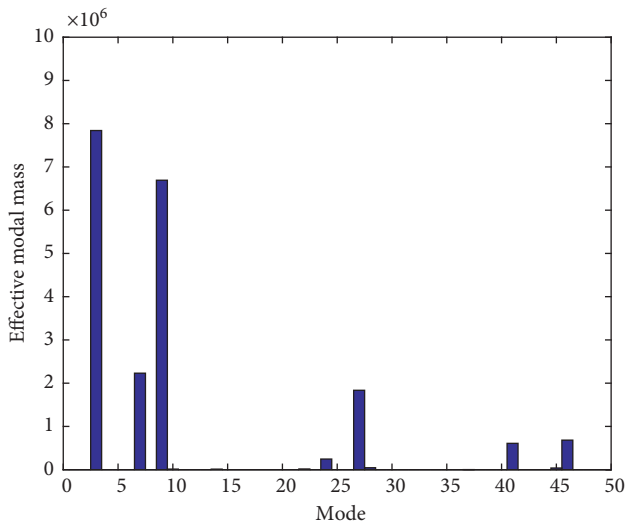

Figure 5: Effective modal mass in y direction.

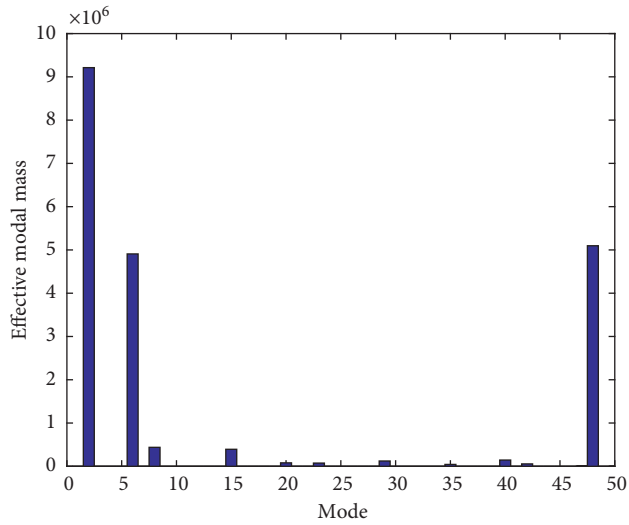

Figure 6: Effective modal mass in z direction.

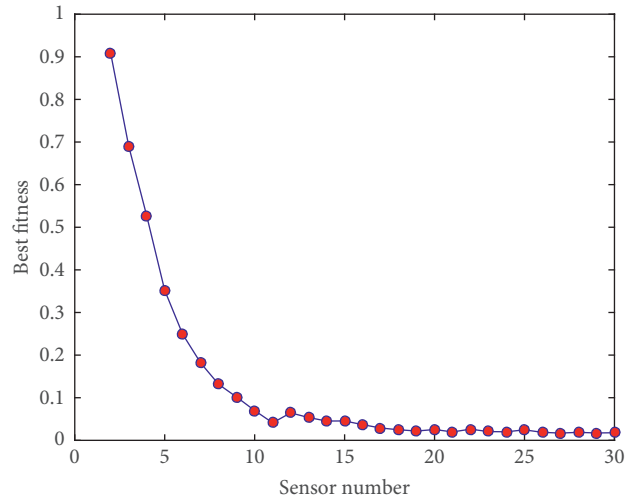

Figure 7: Curve of sensor number.

Table 3: Calculation results based on response of cable-stayed bridge.

Order	Direction	Natural frequency	Modal participation factor	Effective modal mass	r_i in corresponding direction	R in three directions
30	x	5.4742	3258.2	$0.10616E+08$	0.5661	0.1781
2	z	0.7627	3035.3	$0.92131E+07$	0.4477	0.3327
3	y	0.9631	2800.4	$0.78423E+07$	0.3869	0.4643
9	y	1.6349	2587.1	$0.66931E+07$	0.3302	0.5766
48	z	10.295	2257.7	$0.50972E+07$	0.2477	0.6621
6	z	1.2662	2215.5	$0.49084E+07$	0.2385	0.7445
11	x	1.8105	−1498.9	$0.30582E+07$	0.1631	0.7958
16	x	2.6809	−1498.9	$0.22467E+07$	0.1198	0.8335
7	y	1.3117	−1493.8	$0.22314E+07$	0.1101	0.8709
27	y	4.9842	1355.0	$0.18360E+07$	0.0906	0.9017
34	x	6.5904	925.95	$0.85739E+06$	0.0457	0.9161
8	z	1.5352	−662.25	$0.43858E+06$	0.0213	0.9235

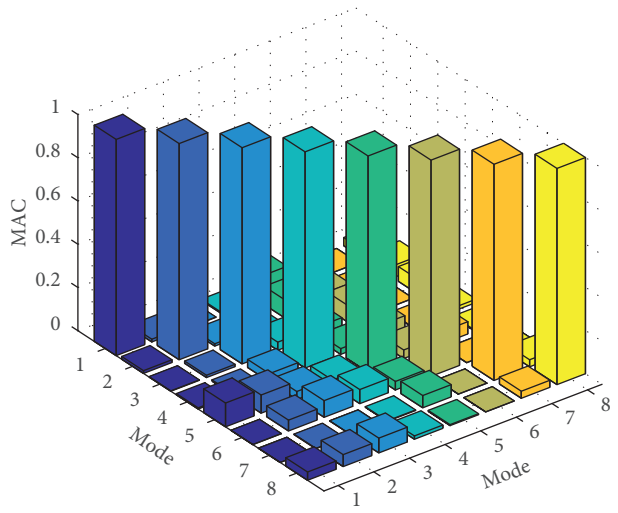

Figure 8: 7-sensor iteration curve.

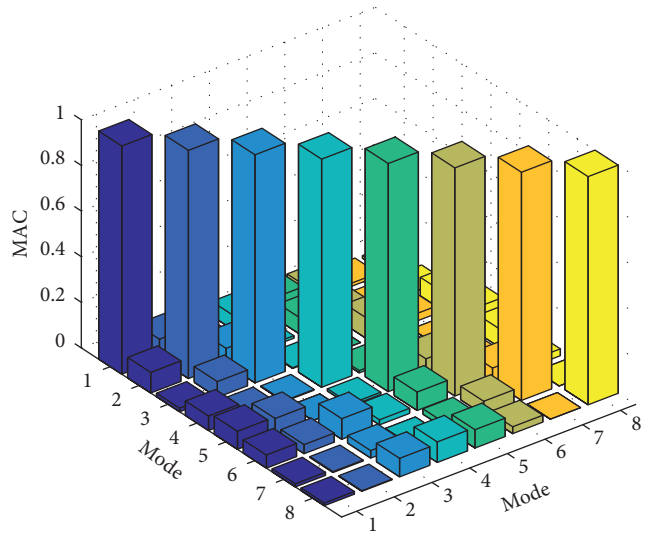

Figure 9: 11-sensor iteration curve.

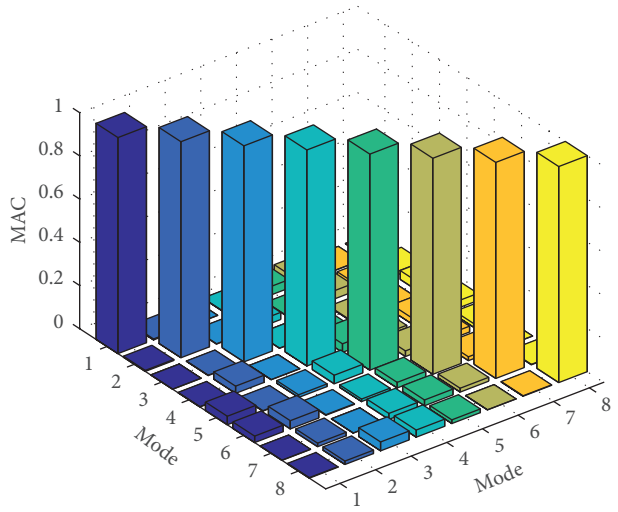

Figure 10: 15-sensor iteration curve.

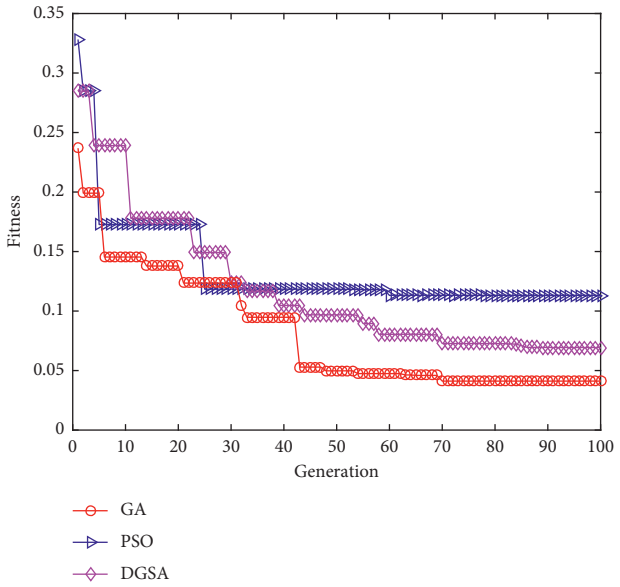

Figure 11: Performance curves of three algorithms.

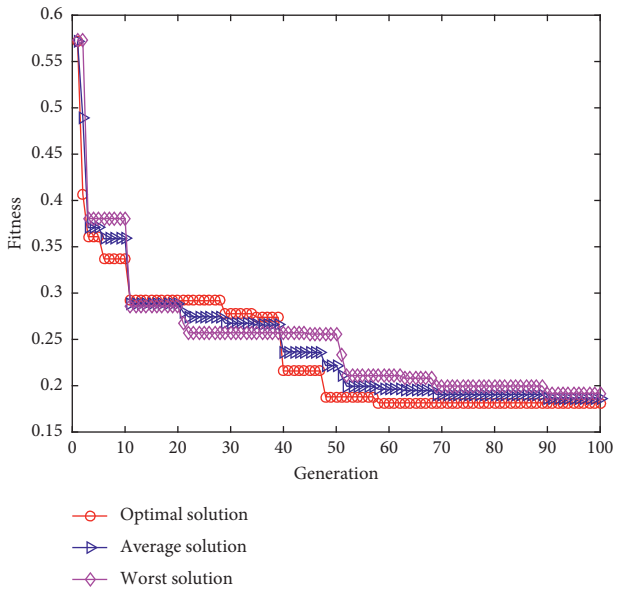

Figure 12: MAC matrix of GA.

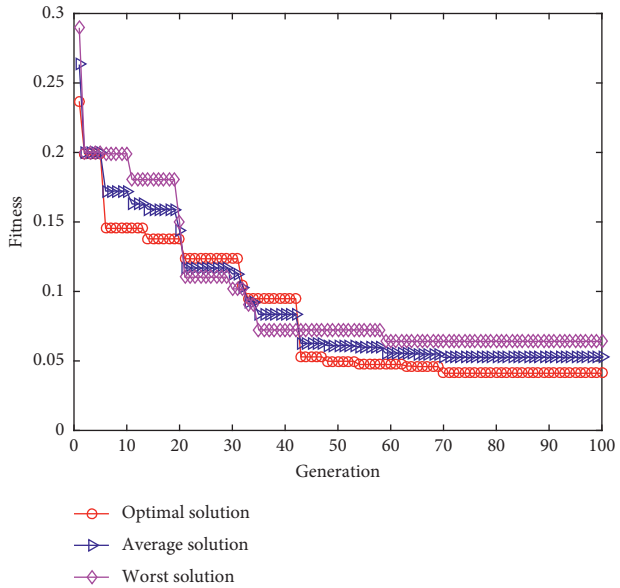

Figure 13: MAC matrix of PSO.

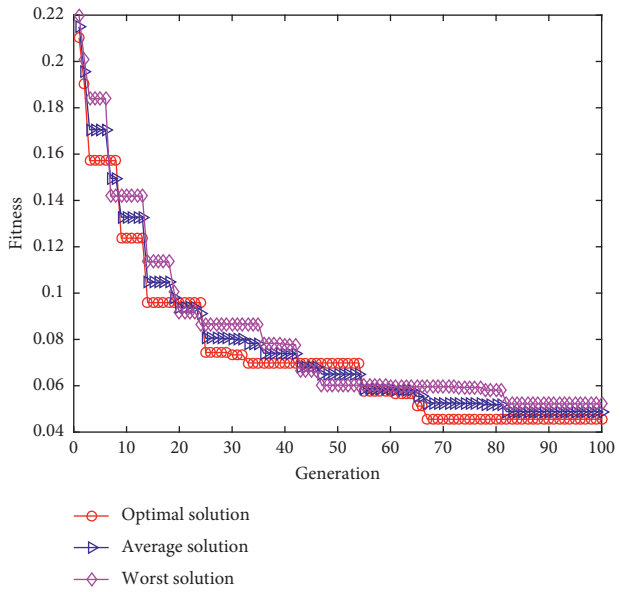

Figure 14: MAC matrix of DGSA.

respectively. Although both values are less than 0.25, there are still cases, wherein it is not possible to distinguish individual locations. However, the maximum value of the off-diagonal element of the DGSA is 0.0410. Considering that the off-diagonal elements of the MAC matrices in Figures 12 and 14 are too small, Figure 15 shows the maximum off-diagonal element of each modal column vector of the MAC matrices corresponding to the three algorithm optimization schemes. We can see that the maximum nondiagonal element in the MAC matrix of DGSA is obviously smaller than the optimal sensor placement value of the GA algorithm and the PSO algorithm. At the same time, from the variation of the curve, we can see that the maximum nondiagonal element variation range for each order mode of the DGSA is smaller, and the result obtained is more stable. This also verifies that the modal vector corresponding to the DGSA offers greater discrimination and a better optimization result.

Figures 16–18 and Tables 4–6 show the optimal sensor placement results and scheme of the three algorithms on the cable-stayed bridge.

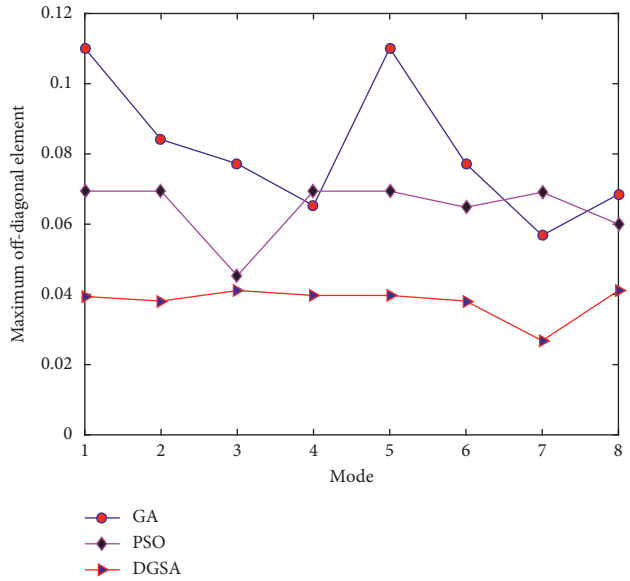

Figure 15: Maximum off-diagonal term at each mode in MAC matrix.

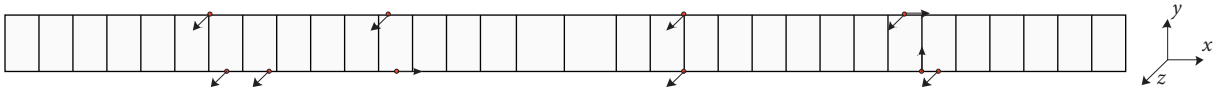

Figure 16: Optimal sensor placement of GA.

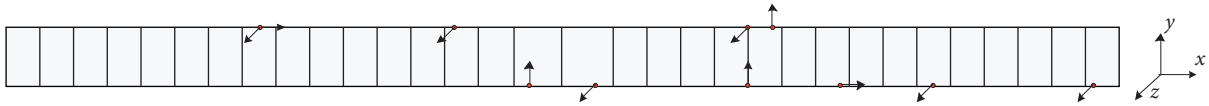

Figure 17: Optimal sensor placement of PSO.

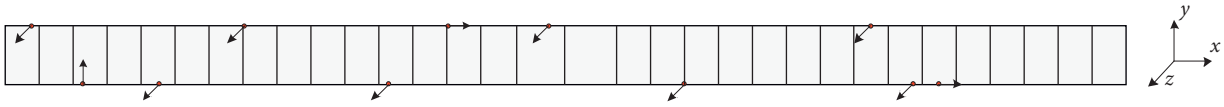

Figure 18: Optimal sensor placement of DGSA.

Table 4: Optimal sensor locations of GA.

Sensor number	1	2	3	4	5	6	7	8	9	10	11
Node	27	27	53	88	109	156	158	186	220	235	240
Direction	x	z	z	z	z	z	y	z	x	z	z

Table 5: Optimal sensor locations of PSO.

Sensor number	1	2	3	4	5	6	7	8	9	10	11
Node	42	45	80	103	103	137	156	167	179	196	204
Direction	y	z	z	x	z	z	z	x	y	z	y

Table 6: Optimal sensor locations of DGSA.

Sensor number	1	2	3	4	5	6	7	8	9	10	11
Node	31	69	81	105	130	156	159	186	221	248	257
Direction	z	z	x	z	z	x	z	z	z	z	y

5. Conclusions and Future Work

This article presents an OSP method based on mode selection and an improved DGSA to solve the sensor placement optimization problem. In order to improve the optimization ability of the algorithm, the DGSA proposed in this paper dynamically adjusts the attenuation factor α.At the beginning of the search, the attenuation factor is small, and the global search step is large. In the later stage of the search, the attenuation factor is larger, and the search step size of the particle is smaller, which is conducive to the algorithm's local search. The modal selection of the initial sensor layout is determined by the experience of the engineer. In this paper, through the calculation of the modal mass participation ratio, the vibration mode, which has a great influence on the bridge's vibration response, is determined, so as to ensure the effectiveness of the selected vibration mode matrix.

The validity and effectiveness of the proposed sensor placement method with DGSA are both demonstrated using the example of a cable-stayed bridge. Compared with the GA algorithm and the PSO algorithm, the sensor placement method based on the DGSA has a greater optimization efficiency and a higher convergence speed, and the optimal placement result is better. In addition, the concept of the DGSA can be applied not only in sensor placement problems but also in similar constrained optimization problems.

Data Availability

The data used to support the findings of this study are available from the corresponding author upon request.

Conflicts of Interest

The authors declare that they have no conflicts of interest.

Acknowledgments

This work was financially supported by the National Key R&D Program of China (Grant no. 2018YFB120602) and the National Natural Science Foundation of China (Grant no. 61463028).

References

[1] J.-F. Lin, Y.-L. Xu, and S. Zhan, "Experimental investigation on multi-objective multi-type sensor optimal placement for structural damage detection," *Structural Health Monitoring*, vol. 18, no. 3, pp. 882–901, 2019.

[2] D. C. Kammer and L. Yao, "Enhancement of on-orbit modal identification of large space structures through sensor placement," *Journal of Sound and Vibration*, vol. 171, no. 1, pp. 119–139, 1994.

[3] Y. Fujino, "Vibration, control and monitoring of long-span bridges-recent research, developments and practice in Japan," *Journal of Constructional Steel Research*, vol. 58, no. 1, pp. 71–97, 2002.

[4] D. C. Kammer, "Sensor placement for on-orbit modal identification and correlation of large space structures," *Journal of Guidance, Control, and Dynamics*, vol. 14, no. 2, pp. 251–259, 1991.

[5] R. Castro-Triguero, S. Murugan, R. Gallego, and M. I. Friswell, "Robustness of optimal sensor placement under parametric uncertainty," *Mechanical Systems and Signal Processing*, vol. 41, no. 2, pp. 268–287, 2013.

[6] T. G. Carne and C. R. Dohrmann, "A modal test design strategy for modal correlation," in *Proceedings of the 13th International Modal. Analysis Conference*, pp. 927–933, Nashville, TN, USA, February 1995.

[7] J. E. T. Penny, M. I. Friswell, and S. D. Garvey, "Automatic choice of measurement locations for dynamic testing," *AIAA Journal*, vol. 32, no. 2, pp. 407–414, 1994.

[8] G. Heo, M. L. Wang, and D. Satpathi, "Optimal transducer placement for health monitoring of long span bridge," *Soil Dynamics and Earthquake Engineering*, vol. 16, no. 7-8, pp. 495–502, 1997.

[9] N. Debnath, A. Dutta, and S. K. Deb, "Placement of sensors in operational modal analysis for truss bridges," *Mechanical Systems and Signal Processing*, vol. 31, pp. 196–216, 2012.

[10] C. Papadimitriou, J. L. Beck, and S.-K. Au, "Entropy-based optimal sensor location for structural model updating," *Journal of Vibration and Control*, vol. 6, no. 5, pp. 781–800, 2000.

[11] H. M. Chow, H. F. Lam, T. Yin, and S. K. Au, "Optimal sensor configuration of a typical transmission tower for the purpose of structural model updating," *Structural Control and Health Monitoring*, vol. 18, no. 3, pp. 305–320, 2011.

[12] T.-H. Yi, H.-N. Li, and M. Gu, "Optimal sensor placement for health monitoring of high-rise structure based on genetic algorithm," *Mathematical Problems in Engineering*, vol. 2011, Article ID 395101, 12 pages, 2011.

[13] C. He, J. Xing, J. Li, and Q. Yang, "A new optimal sensor placement strategy based on modified modal assurance criterion and improved adaptive genetic algorithm for structural health monitoring," *Mathematical Problems in Engineering*, vol. 2015, Article ID 626342, 10 pages, 2015.

[14] T.-H. Yi, H.-N. Li, G. Song, and X.-D. Zhang, "Optimal sensor placement for health monitoring of high-rise structure using adaptive monkey algorithm," *Structural Control and Health Monitoring*, vol. 22, no. 4, pp. 667–681, 2015.

[15] H. Jin, J. Xia, and Y.-Q. Wang, "Optimal sensor placement for space modal identification of crane structures based on an improved harmony search algorithm," *Journal of Zhejiang University*, vol. 16, no. 6, pp. 464–477, 2015.

[16] H. Yin, K. Dong, A. Pan, Z. Peng, Z. Jiang, and S. Li, "Optimal sensor placement based on relaxation sequential algorithm," *Neurocomputing*, vol. 344, pp. 28–36, 2019.

[17] X. Zhang, J. Li, J. Xing, and P. Wang, "Optimal sensor placement for latticed shell structure based on an improved particle swarm optimization algorithm," *Mathematical Problems in Engineering*, vol. 2014, Article ID 743904, , 2014.

[18] W. Deng, "Differential evolution algorithm with wavelet basis function and optimal mutation strategy for complex optimization problem," *Applied Soft Computing*, Article ID 106724, 2020.

[19] G.-D. Zhou, T.-H. Yi, H. Zhang, and H.-N. Li, "A comparative study of genetic and firefly algorithms for sensor placement in structural health monitoring," *Shock and Vibration*, vol. 2015, Article ID 518692, 10 pages, 2015.

[20] J. Li, X. Zhang, J. Xing, P. Wang, Q. Yang, and C. He, "Optimal sensor placement for long-span cable-stayed bridge using a novel particle swarm optimization algorithm," *Journal of Civil Structural Health Monitoring*, vol. 5, no. 5, pp. 677–685, 2015.

[21] E. Rashedi, H. Nezamabadi-pour, and S. Saryazdi, "A gravitational search algorithm," *Information Sciences*, vol. 179, no. 13, pp. 2232–2248, 2009.
[22] T. W. Saucer and V. Sih, "Optimizing nanophotonic cavity designs with the gravitational search algorithm," *Optics Express*, vol. 21, no. 18, pp. 20831–20836, 2013.
[23] P. Niu, C. Liu, P. Li, and G. Li, "Optimized support vector regression model by improved gravitational search algorithm for flatness pattern recognition," *Neural Computing and Applications*, vol. 26, no. 5, pp. 1167–1177, 2015.
[24] F. Chen, J. Zhou, C. Wang, C. Li, and P. Lu, "A modified gravitational search algorithm based on a non-dominated sorting genetic approach for hydro-thermal-wind economic emission dispatching," *Energy*, vol. 121, pp. 276–291, 2017.
[25] D. C. Kammer and M. L. Tinker, "Optimal placement of triaxial accelerometers for modal vibration tests," *Mechanical Systems and Signal Processing*, vol. 18, no. 1, pp. 29–41, 2004.
[26] L. Zhang, Y. Xia, J. A. Lozano-Galant, and L. Sun, "Mass-stiffness combined perturbation method for mode shape monitoring of bridge structures," *Shock and Vibration*, vol. 2019, Article ID 7320196, 14 pages, 2019.
[27] T.-H. Yi, H.-N. Li, and M. Gu, "Optimal sensor placement for structural health monitoring based on multiple optimization strategies," *The Structural Design of Tall and Special Buildings*, vol. 20, no. 7, pp. 881–900, 2011.